

EV Charging Through Three-Port Wireless Power Transfer

S.Bhagyashri, Kanimozhi.G

Abstract: Electric vehicle are gaining importance day by day because of the benefits it has over conventional vehicles. As a future response for Electric Vehicle (EV) charging practicality of Contactless Power Transfer (CPT) is being explored broadly for past couple of years. The primary snags in CPT are cost, range, misalignment tolerances and low power efficiency. By introducing Wireless Power Transfer (WPT) in EVs, the drawbacks such as charging time, range, and cost can be successfully moderated. WPT is a potential alternative in EV to overcome plug-in problems. This paper currently discusses about the recent technical advancements in EVs and problems faced by implementing WPT. With many recent advances in WPT makes it very desirable to EV applications, in both dynamic charging and stationary charging circumstances which eliminates the bulky, heavy battery requirements. This paper discusses about the 2 port and 3 port WPT mostly used for EV. MATLAB-Simulink Software and PSIM Software are used to analyze the WPT. Future technologies such as Wireless Electric Vehicle Charging Systems (WEVCS) such as "Vehicle to Grid (V2G)" charging systems are also discussed with comparisons among the existing technologies.

Index terms: Wireless Charging, WPT, Inductive Charging, Vehicle Charging, Electric Vehicle

I. INTRODUCTION

EV has seen many advancement and innovations over a decade. EV is a potential alternative to the conventional gasoline vehicles which emits carbon dioxide causing pollution to the environment. EVs also eradicates the threat of depleting natural resources, when compared to the conventional vehicles which uses petrol or diesel that gets depleted over a period of time. Many EVs such as Plug-in Electric Vehicle (PHEVs) are introduced to the market. Despite government subsidy and tax waver, EVs are less attractive choice to the consumer due to major drawbacks in the energy storage technology.

Furthermore, connecting the plug every time for charging may annoy an EV client. Remote power exchange innovation is considered as a compelling method to take care

of this issue. By introducing WPT, an electric vehicle can accomplish opportunity charging [1]. The most normal approach to acknowledge WPT at exhibit is inductive power exchange innovation, which comprises of a transmitting loop and a receiving loop. Through electromagnetic field, the power can be transferred wirelessly. Eliminating the use of the wiring, the power transfer process is simplified. Wireless power transfer(WPT) suggests an alluring other option to a conventional charging framework. The driver is expected to stop their vehicle over a (Transmission loop) Tx loop inserted in the ground, permitting the case mounted (Receiver Loop) Rx curl to charge [2]. WPT innovation can be utilized as response to eliminate many charging risks and increases effective driving range. The dynamic WPT allows the EVs to charge while the vehicle is still moving on the road, this improves the viable driving extent at the same diminishing the battery size stockpiling. WPT powered EVs proves to be extremely useful from customer's perspective. For instance, the implementation of V2G [3] proves to be a promising future solution that can be carried into next stage with WPT stimulated EVs [4]. Introduction of wireless charging has led to shrinking of battery size by 20% when compared to EVs operating with conductive charging. This paper presents the comparison of 2 ports and 3 port wireless inductive power transfer and the simulation results of the two in brief.

II. BASICS OF WPT:

To transfer electrical power from the power source to load without any physical contact is known as WPT. Introduction to Maxwell's theories in 1862 marked the beginning of WPT. Later in 1884, the hypothesis proposed by Henry Poynting described the electromagnetic waves as a flow of energy. At the beginning of twentieth century, Nikola Tesla discovered the standards of WPT [5]. Due to the low productivity, safety, and money related imperatives, the use of Tesla's invention was unable to be utilized in business level markets. With the recent semiconductor advancements, Tesla's experiments have turned into a reality. The wireless transmission is more advantageous where execution of physical connectors can be complex, risky or incomprehensible, especially in EVs. The block diagram of static WPT in EV is illustrated in Fig1. To enable power transfer from transmission coil to receiver coil, The AC source from the grid is converted into High Frequency (HF) AC by AC-DC and DC-AC converter setup. The efficiency of the system is improved by introducing series and parallel combination of compensation network in both transmitting and receiving side. Receiving coil is mounted underneath the vehicle which converts oscillating magnetic field into HFAC.

Revised Manuscript Received on 22 May 2019.

* Correspondence Author

S.Bhagyashri*, School of Electrical Engineering, Vellore Institute of Technology, Chennai, Tamil Nadu, India.

Kanimozhi.G, School of Electrical Engineering, Vellore Institute of Technology, Chennai, Tamil Nadu, India.

© The Authors. Published by Blue Eyes Intelligence Engineering and Sciences Publication (BEIESP). This is an [open access](https://creativecommons.org/licenses/by-nc-nd/4.0/) article under the CC-BY-NC-ND license <http://creativecommons.org/licenses/by-nc-nd/4.0/>

HFAC is converted into stable DC and stored in battery bank or BMS (Battery Management System). For ensuring stable operation and to elude safety and health constrains, BMS is also installed. To improve magnetic flux distribution and reduce any harmful flux leakages, magnetic planar ferrite plates are employed in either side.

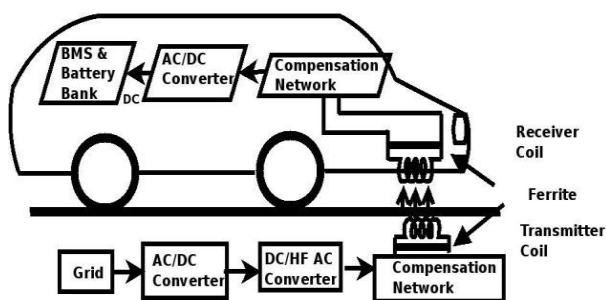
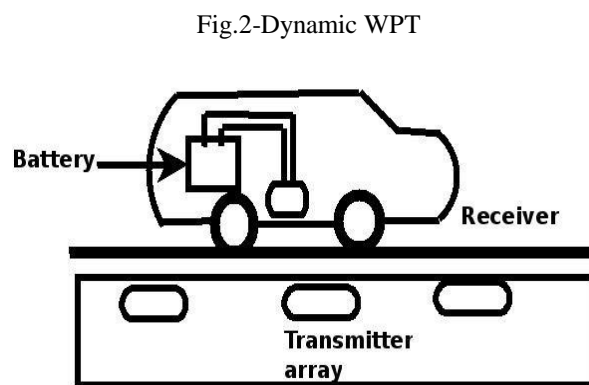


Fig.1- Block diagram of static WPT in EV

a. Dynamic WPT for wireless charging :

With implementing the dynamic WPT in EVs, the EV is charged while the vehicle is continuously moving. WPT increases the driving range of EVs and reduces the battery size. However, implementation of sophisticated system dependent on the infrastructural advancement and cost. The power level if the system, vehicle speed and duration of travel determines the amount of energy gained by WPT. Segmented transmitter coil array and single transmitter configuration are the two types of transmitter array configuration of dynamic charging methodologies. The single transmitter track configuration comprises of a power source connected with long transmitter coil track. The receiver is detectably smaller than the length of the track. Multiple coils with high frequency power sources are introduced in segmented coil array-based method. This is illustrated in Fig. 2. As the tracks in transmitter-based framework is powered from solitary sources [6],[7], the control of WPT is less demanding. When the vehicle moves along the track coupling coefficient is nearly constant. The length of transmitter track is usually few meters to several meters in length. Though this kind of configuration experiences a few disadvantages. The electromagnetic field discharged inside the uncoupled parts must be suppressed to wipe out harmful exposure. Also, to compensate huge inductive effect, the compensation capacitor is connected along the track. This introduces extra constrain in development. When the transmitter area secured by receiver is lesser, the coupling coefficient is lesser resulting in lower efficiency. Magnetic flux is increased, and effectiveness is enhanced by using ferromagnetic materials. Relative range of track-based network is considerably lesser than solidarity. The requirement of distributed compensation and field exposures are eliminated in the segmented coil array methodology while lowering the coupling issues. However, it induces many other designing trials. As the load moves along the array, it is vital to align the receiver and the transmitter positions and switch the appropriate power supply. And moreover, the separation between the transmitter and receiver coil needs to be optimized. The efficiency reduces steeply as the space between the coils increases. There is a dip in continuity

when receiver moves away from transmitter power supply. However, the closeness of two coils introduces some problems. Primarily, the negative current stress is generated between adjacent transmitter coils due to negative mutual inductance. Many transmitters introduced in the track increases the designing cost. Multiple coil connection with source converters also poses a major drawback. Each coil may be connected to a converter or a single power converter can related to several transmitter coils.



b. Analysis of telemetry system:

The gap between the coils and mutual coupling mainly determines the power received in receiver's side. Two coils are said to be inductively linked when the external source excites the primary coil, which in turn induces magnetic field in secondary coil producing the voltage across the terminals. The overall performance of the system is decided by positioning and dimensions of coils. Mutual coupling can be expressed as

$$M = \frac{\mu_0 \pi N_1 R_1^2 N_2 R_2^2}{\sqrt{(R_1^2 + x^2)^3}} \quad (1)$$

Where M is the mutual coupling coefficient.

μ_0 =Permeability of air ($4\pi \times 10^{-7} \text{ Hm}^{-1}$)

N_1 = Turns in primary coil

R_1 =Radius of coil in source loop in m

N_2 =Turns in secondary coil R_2 =Radius of coil in load loop in m x = Separation between the coil in m As the separation between the coil increases, it is perceived that the mutual inductance M reduces remarkably. Coil need to be placed near each other for higher values of M. The coupling coefficient K is determined

$$K = \frac{M}{\sqrt{L_1 L_2}} \quad (2)$$

where L_1 = self-inductance of coil 1 and L_2 = self-inductance of coil 2 respectively.

c. Modeling of two coil inductive coupling:

The mutual coupling between two coil separated by a certain distance is $j\omega M$. The coil connected to source is source coil and coil connected to load is load coil. The circuit shown in Fig-3 uses inductive coupling WPT. Currents for the loop can be calculated by using KVL.



$$I_1 = \frac{\begin{vmatrix} V_s & -j\omega M \\ 0 & Z_{22} \end{vmatrix}}{\begin{vmatrix} Z_{11} & -j\omega M \\ -j\omega M & Z_{22} \end{vmatrix}} = \frac{V_s Z_{22}}{Z_{11} Z_{22} + \omega^2 M^2} \quad (3)$$

$$I_2 = \frac{\begin{vmatrix} Z_{11} & V_s \\ -j\omega M & 0 \end{vmatrix}}{\begin{vmatrix} Z_{11} & -j\omega M \\ -j\omega M & Z_{22} \end{vmatrix}} = \frac{j\omega M V_s}{Z_{11} Z_{22} + \omega^2 M^2} \quad (4)$$

Power sent from source loop to load loop is given by,

$$P_{transferred} = |I_1| V_s \quad (5)$$

$$P_{received} = |I_2|^2 R_1 \quad (6)$$

The effective power is,

$$P_{eff} = \frac{P_{received}}{P_{transferred}} * 100 \quad (7)$$

Substituting equation (5) and (6) in equation (7)

$$P_{eff} = \frac{|I_2|^2 R_1}{|I_1| V_s} * 100 = \frac{\omega^2 M^2 R_1}{|Z_{22} Z_{11} + \omega^2 M^2|} * 100 \quad (8)$$

d. Modeling of 3 coil inductive coupling:

The three port inductive coil energy transferring system consist of a source loop with primary coil, load loop with secondary coil a hub loop containing a coil which acts as a link between the primary and secondary coil. Two coupling coefficients are jM1 and jM2. Assuming the impedance in source loop to be Z11, hub loop as Z22 and load loop as Z33, the current in three loops are given by

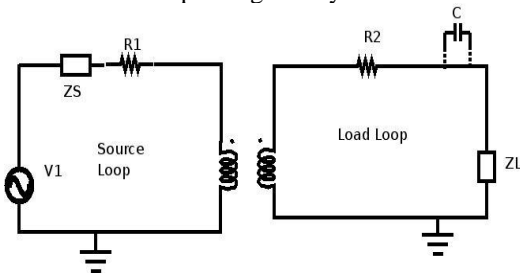


Fig 3. The 2 port WPT

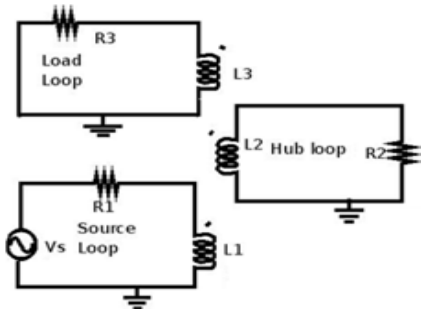


Fig 4. The 3 port WPT

$$I_1 = \frac{V_s (Z_{22} Z_{33} + \omega^2 M^2)}{Z_{11} (Z_{22} Z_{33} + \omega^2 M^2) + \omega^2 M_1^2 Z_{33}} \quad (9)$$

$$I_2 = \frac{V_s (j\omega M_1 Z_{33})}{Z_{11} (Z_{22} Z_{33} + \omega^2 M^2) + \omega^2 M_1^2 Z_{33}} \quad (10)$$

$$I_3 = \frac{V_s (M_1 M_2 \omega^2)}{Z_{11} (Z_{22} Z_{33} + \omega^2 M^2) + \omega^2 M_1^2 Z_{33}} \quad (11)$$

Where I1, I2 & I3 are current through source loop, hub loop and load loop respectively. Vs are the source voltage connected to source loop.

Power transferred and power received are given by,

$$P_{transferred} = |I_1| V_s \quad (12)$$

$$P_{received} = |I_2|^2 R_1 \quad (13)$$

Where R1 is the resistance in load loop.

From equation (12) and (13) the total power efficiency is,

$$P_{eff} = \frac{V_s (\omega^2 M_1^2 M_2^2)}{(Z_{22} Z_{33} + \omega^2 M^2)} \dots \dots \dots (14)$$

e. Design of WPT model:

MATLAB Simulink was used to design the WPT. The design of the WPT is shown in Fig 5. 230 V, 50Hz AC voltage is given to bridgeless interleaved PFC boost converter which boosts the voltage to 400V and converts it to DC, which is in turn fed to Single phase full bridge inverter. Inverter converts DC voltage to high frequency AC voltage of 400V with switching frequency 100 kHz. The high frequency AC is transmitted from primary coil to secondary coil with the help of hub loop. The transmitted AC voltage is fed to rectifier which converts AC to DC which is then fed to the load or the battery inside the car.

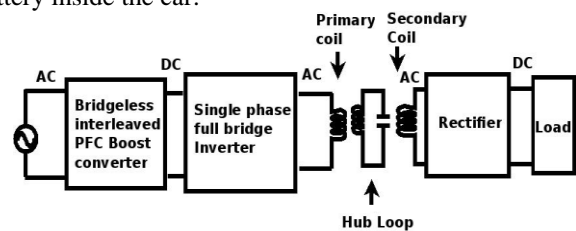


Fig 5-Design of WPT model

Bridgeless interleaved PFC boost converter:

This AC/DC converter has reduced input current ripple with minimum inductor volume and cost. The BLIL boost converter shown in Fig 6 has increased efficiency, increased output voltage, more reliability and fewer ripples as compared to interleaved boost converter. To ensure interleaving the, the firing pulses to the switches are given in 180° phase shift. The converter proposed has four switches (Q1-Q4). The operation of this converter is discussed in two half cycles. During positive half cycle of AC input voltage, trigger pulses are given to Q1/Q2. The current flow is through L1-Q1-Q2-L2. When switches Q1/Q2 are turned off, the energy stored in L1, L2 are released through diode D1. Similarly, current flows through L3-Q3-Q4-L4, when pulses (with 180° phase shift) are given to Q2/Q4. Energy stored in L3, L4 is released through D3. During negative half cycle, the current flows through L2-Q2-Q1-L1. The stored energy in inductor L2 and L1 is released through D2. Similarly, L3-Q3-Q4-L4 is the order of current flow when pulses (with 180° phase shift) are given to Q2/Q4. Energy stored in L3, L4 is released through D4.

The output voltage is given by

$$V_o = \frac{1}{1-D} V_{in} \quad (15)$$

Where Vin is the input voltage.

Output ripple current is given by,

$$\Delta I_{rp} = \frac{I_p}{2} \quad (16)$$

Where Ip is peak current. Voltage across semiconductor device is given by,

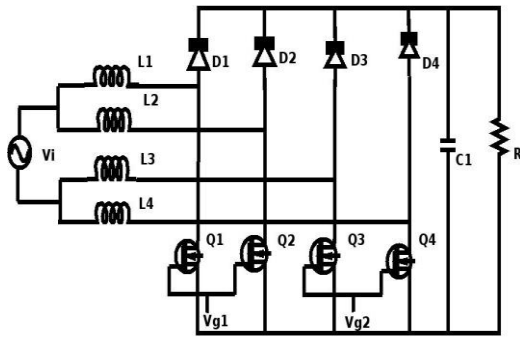


Fig 6 - Bridgeless interleaved PFC boost converter

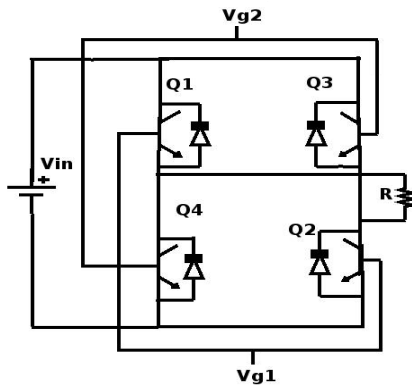


Fig 7-Single phase full bridge inverter.

$$V_{sc} = GV_{in} = V_o \tag{17}$$

Where gain, $G = \frac{V_o}{V_{in}}$. The inductor current is given by,

$$\Delta I_L = \frac{V_p \sqrt{2D}}{f_s L/2} \tag{18}$$

Where V_p is peak voltage and f_s is switching frequency in kHz and L is the inductor value in mH.

Single phase full bridge inverter shown in Fig 7 converts DC to AC. This is a high frequency inverter. Q1 and Q2 are operated for duration $0 < t < T_1$, input voltage V_{in} appears across the load. V_{g2} pulses with 180° phase shift are given to Q3 and Q4. The current flows through V_{in} -Q3-R-Q4- V_{in} .

III SIMULATION RESULTS:

The analysis focuses on two element system of spiral resonators [8]. The spiral geometry for 10 MHz system is shown in Fig 8. The magnetic field, being the dominant field of the resonator is plotted in Fig 9. The wireless ports are modelled in linear way to have maximum power transfer. The wireless power transfer comprises of two parts Tx and Rx which is represented in Fig-10. Peak efficiency occurs when the system is operating at resonant frequency. The frequency vs magnitude graph is given below in Fig 11. The coupling increases with decreasing distance between the resonator coils. The magnitude, distance and frequency plot are shown in Fig 12. The magnetic resonant energy exchange mechanism between two coils is shown in Fig 13.

The input waveform of the WPT is power factor corrected and is shown in Fig.14. The power factor of AC input is maintained closer to unity. The output waveform of voltage acquired is presented in Fig.15. The 230 V input is boosted and converted to DC by PFC boost rectifier to 400V.

The gating pulse is provided to the inverter with 180° -degree phase shift as depicted in Fig 16. The inverter input voltage in Fig.18 is given as a DC input to the inverter from the PFC converter.

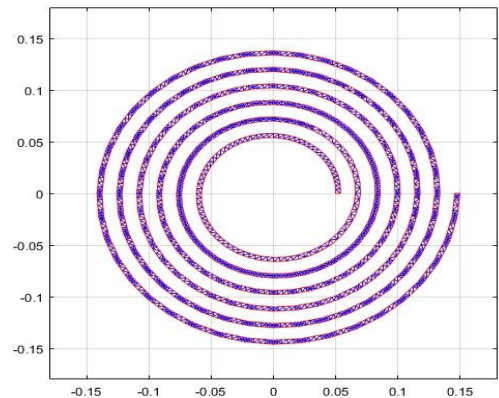


Fig.8 Spiral geometry of WPT

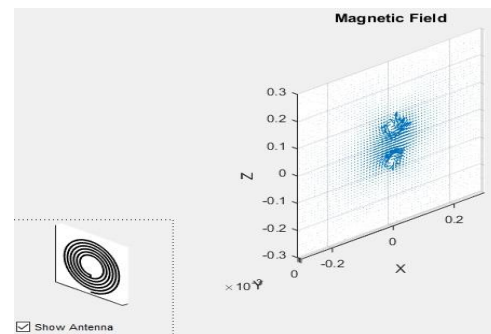


Fig.9 The magnetic field distribution

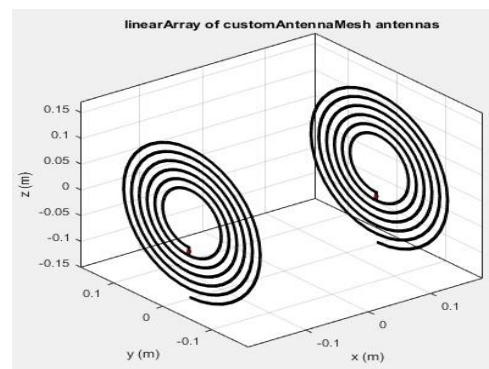


Fig.10 Linear array of WPT

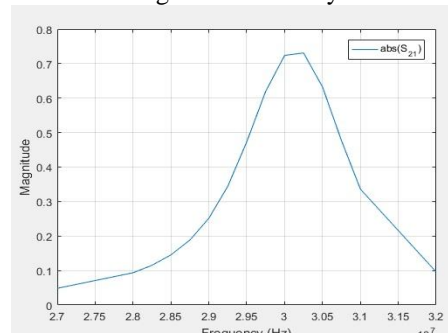


Fig.11 Maximum power transfer

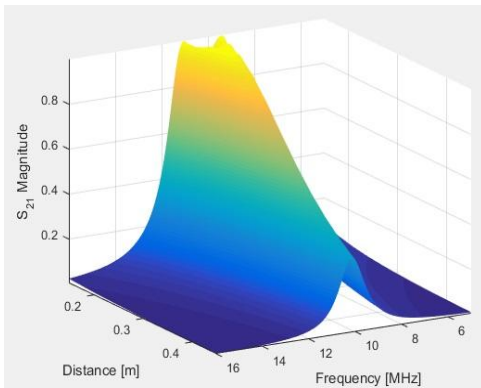


Fig.12 Distance, Magnitude, Frequency relation in WPT

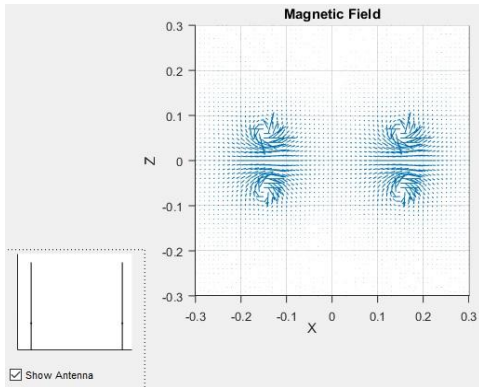


Fig.13 Magnetic field between coils

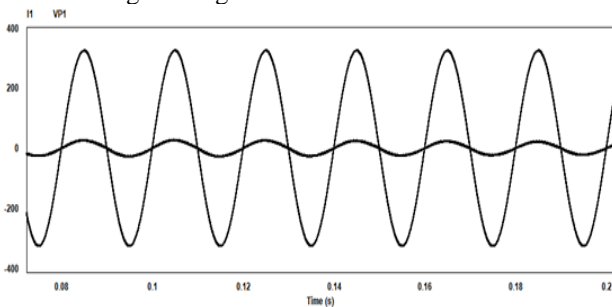


Fig14: Input voltage and Input Current waveform

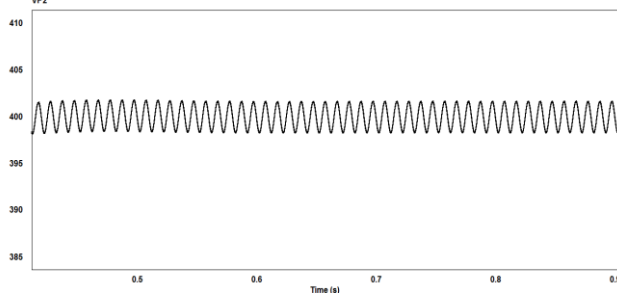


Fig 15- Output voltage waveform from the PFC boost converter

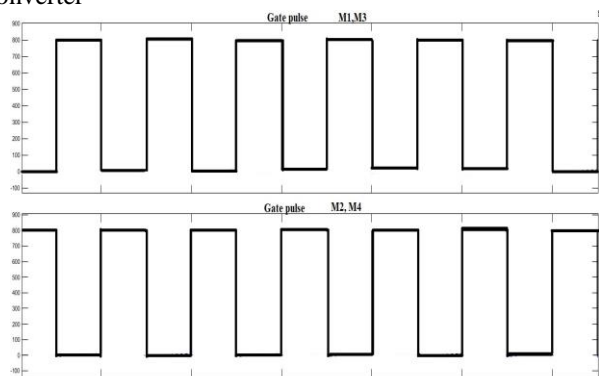


Fig 16- Gating Pulses given to the inverter and the converter in the design

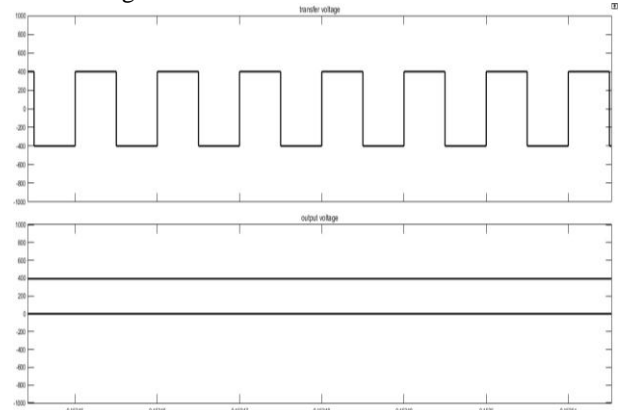


Fig 17: (a) Voltage across receiver loop (b) output voltage

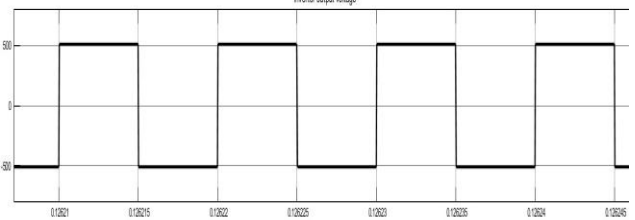


Fig 19: Inverter output voltage waveform

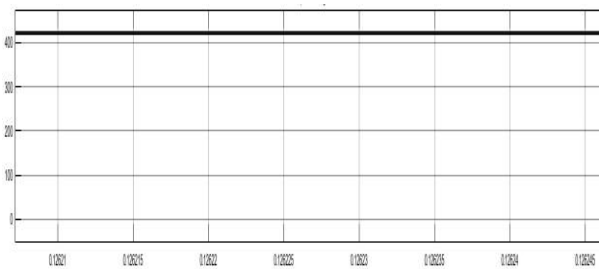


Fig 20: Output voltage from diode bridge rectifier

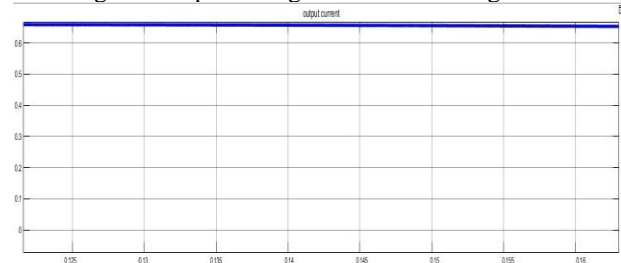


Fig 21: Output current

The inverter output voltage shown in Fig 19 is transferred in the form of high frequency AC by inverter. The high frequency AC voltage fed to the primary coil. The secondary coil receives the AC voltage and fed to the diode bridge rectifier. The rectifier converts AC to DC and obtained output voltage of the rectifier is shown in Fig 20. The output voltage of 400V DC is used for electric vehicle charging. The output voltage and current is shown is Fig 17(b) and Fig 21 respectively. Fig-22 shown above realizes the efficiency vs. load curve. The efficiency increases with increase in load till full load operation. It is realized that efficiency of 3port WPT is greater than efficiency of 2 port WPT. WPT is more efficient with 3 port power transfer than 2 port WPT.

IV. WIRELESS VEHICLE TO GRID (W-V2G)- FUTURE APPLICATION:

The development and advancement in EVs have resulted in efficient charging techniques and wireless transfer. Power requirements from distribution networks have increased with the increased number of PEVs and had created detrimental impact on it. In the view of compensating high power demands, Renewable energy sources (RES) and Distributed Generation (DG) have been introduced to micro grid. But introduction to such new techniques have limited support facilities. Advanced scheduling for charging and discharging to distribution network is introduced by vehicle to grid (V2G). The most common application is the bidirectional power transfer in PEVs with wireless plug-in. During peak times, the onboard bidirectional charger allows the user to connect to the grid. The vehicles charge from the power socket during off- peak times. To ensure safety for the user AC-DC conversion takes place before it is fed to isolated DC-DC converter. The rippled DC is again fed to DC-DC converter before storing it in battery through BMS.

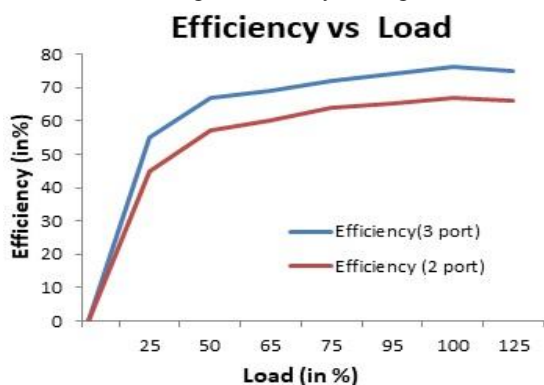


Fig 22- Load Vs Efficiency

The buck mode operation happens when the battery bank is charged, and boost mode operation happens when the battery discharges. The major drawback of this method illustrated in Fig 22(b) is manual intervention and physical contact to charge and discharge the EVs which create further hazards such as electric shocks and trip risks. A wireless V2G is illustrated in Fig 22(a). The primary side of wireless transmission is implanted on roads and parking areas unlike the plug in V2Gs shown in Fig 22(b). With other power converter devices mounted on the body of the car, the receiver coil is installed beneath the EV. The completely automotive design structure with the wireless transformer provides additional isolation between the source and receiver side. The design topology receives energy to rectify peak demand in static and dynamic modes with reduced stress and provides surplus energy to transfer.

V. CONCLUSION

This paper presents the comprehensive view of WPT their application in modern trends and the usage in EVs. The usage of rectifier, PFC converter, and inverter has increased the efficiency of power transferred wirelessly.

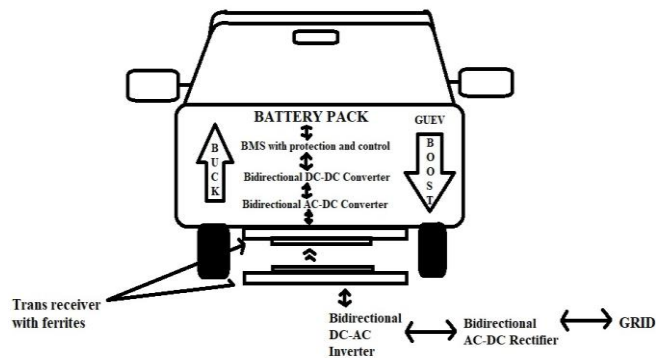


Fig 22(a) Bidirectional wireless V2G

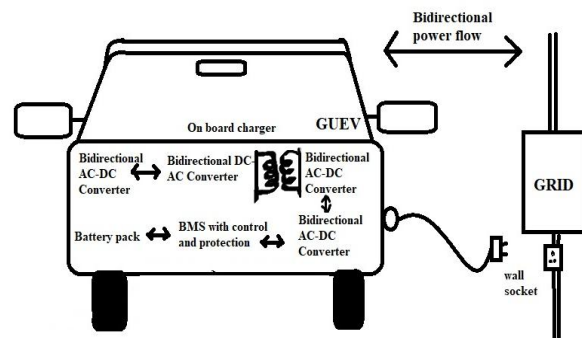


Fig 22(b) Bidirectional plug-in V2G

This paper also highlights the derivations of 3 coils and 2 coil WPT topologies used in common. From the simulation results and past researches, it is evident that 3 coil WPT is more efficient than 2 coil WPT topology. This paper also highlights the topology and design of converter and inverter used for WPT. Resonant coupled WPT is also analyzed. A bidirectional WPT system can charge and discharge EVs in future implementation, which provides greater flexibility, convenience, less cost and increases stability of the grid. Advancements such as dynamic WPT by constructing power tracks proves to be cost effective as compared to hybrid plug in EV charging. With advancement of semiconductor switches, control topologies and protection system of power grid, WPT is made possible and feasible in near future.

REFERENCES

1. S. Lukic and Z. Pantic, "Cutting the cord: static and dynamic inductive wireless charging of electric vehicles," in *IEEE Electrification Magazine*, vol. 1, no. 1, pp. 57-64, Sept. 2013.
2. S.A.Birrell, "How driver behavior and parking alignment affects inductive charging systems for electric vehicles," *Transp. Res. Part C, Emerg. Technol.*, vol. 58, Part D, pp. 721-731, 2015.
3. Madawala UK, Schweizer P, Haerri VV, "Living and mobility—a novel multipurpose in-house grid interface with plug in hybrid blue angle", presented at the *IEEE international conference on sustainable energy technologies*, 2008.
4. Madawala UK, Thrimawithana DJ, "A bidirectional inductive power interface for electric vehicles in V2G systems," *IEEE Trans Ind Electron* 58:789-4796
5. Tesla N, Apparatus for transmitting electrical energy. US patent 1,119,732, December 1914.
6. J.L.Villa, J.Sallan, J.F.S Osorio, A.Lobmbart,, "High-misalignment tolerant compensation topology for ICPT Systems," *IEEE Trans.Indust.Electr.* vol 59,2012 pp-945-951.
7. K.Kalwar, S.Mekhilef, M.Seyedmahmoudian, B.Horan, "Coil design for high misalignment tolerant inductive power transfer system for EV charging", *Energies*, vol 9,2016, 937.



8. Shriniketh C.M and Kanimozhi.G," Implementation of ZVS in an interleaved boost rectifier", *International Journal of Applied Engineering Research*, Vol. 10 No.20 ,2015, pp. 15852-15857.
9. Tanima kar and Kanimozhi.G, "Modeling and Analysis of Modified Bridgeless Pseudo-Boost Converter," *International Journal of Control Theory and its Applications*, Vol.9, Issue.7, 2016, pp.3315-3326.
10. Kanimozhi G and Sreedevi V.T, "Improved resettable integrator control for a bridgeless interleaved AC/DC converter," *Turkish Journal of Electrical Engineering & Computer Sciences*, 2017, Vol.25, no.5, pp:3578 - 3590.
11. Kanimozhi.G and Sreedevi.VT," Semi bridgeless Interleaved PFC Boost Rectifier for PHEV Battery chargers", *IETE Journal of Research*, Taylor and Francis, vol.65, issue.1 pp-128-138.
12. A. P. Sample, D. T. Meyer, and J. R. Smith, "Analysis, Experimental Results, and Range Adaptation of Magnetically Coupled Resonators for Wireless Power Transfer", *IEEE Transactions on Industrial Electronics*, vol 58 (2) 2011, pp.544-554.

AUTHORS PROFILE



S.Bhagyashri is perusing her Bachelor's degree in Electrical and Electronics Engineering in VIT Chennai from 2015. Her research interest includes power electronics converters, and electromagnetics.



Kanimozhi.G received her Bachelor of Engineering from Bharathiyar University, Master of Engineering from Anna university and her Ph.D from VIT University, Chennai. She is working as Assistant Professor (Selection Grade) in the School of Electrical Engineering, VIT Chennai. Her research area includes AC-DC converters for Electric vehicles, Electromagnetics, Multilevel inverters and DC-DC resonant converters.